

A New Intracrystalline Isotope Effect: ^{18}O under the Faces of Amethyst

A. Klemm

Max-Planck-Institut für Chemie (Otto-Hahn-Institut), Mainz

A. Banerjee

Institut für Geowissenschaften der Universität Mainz

S. Hoernes

Mineralogisch-Petrologisches Institut der Universität Bonn

Z. Naturforsch. **45a**, 1374–1376 (1990); received November 15, 1990

The concentration of ^{18}O within well formed crystals of amethyst was found to vary beneath the different growth faces, increasing in the order $z \rightarrow r \rightarrow m$. The $^{18}\text{O}/^{16}\text{O}$ fractionation factor between the faces m and z was measured as 1.0007.

Introduction

Intracrystalline isotope effects have rarely been studied. Reference [1] deals with such an effect in $\text{CuSO}_4 \cdot 5 \text{H}_2\text{O}$.

In the present work it is examined if during the growth of quartz, different amounts of ^{18}O are incorporated at its structurally differing faces z , r and m . These faces are illustrated in Fig. 1, which is a projection perpendicular to the c -axis and parallel to two opposite m -faces [2]. Evidently the arrangement of Si and O exposed to the mother fluid is different for the faces z , r , and m . (The structure of the two m faces in the figure differs in orientation only.) Possible positions (sites) of SiO_2 units attaching during growth are also shown in the figure.

Because of the structural differences of the faces, the growth rate on the faces increases in the order $m \rightarrow r \rightarrow z$ and the amount of impurities incorporated increases in the order $m \rightarrow z \rightarrow r$ [3]. These rules are, however, not always obeyed because other, accidental factors play also a role, e.g. the kind of convection of the mother fluid around the growing crystal. One therefore cannot expect to find strict laws for the incorporation of ^{18}O at the faces of crystals grown in nature but rather trends as for the growth rates and impurity incorporations.

One factor which can be excluded in the comparison of the faces is the variation in time of the temper-

ature and composition of the mother fluid from which the crystal has grown. This can be done by taking the samples to be compared from the same mantle zones, i.e. zones which have grown during the same time span. Mantle zones can be distinguished in the coloured varieties of quartz (smoky quartz, amethyst,

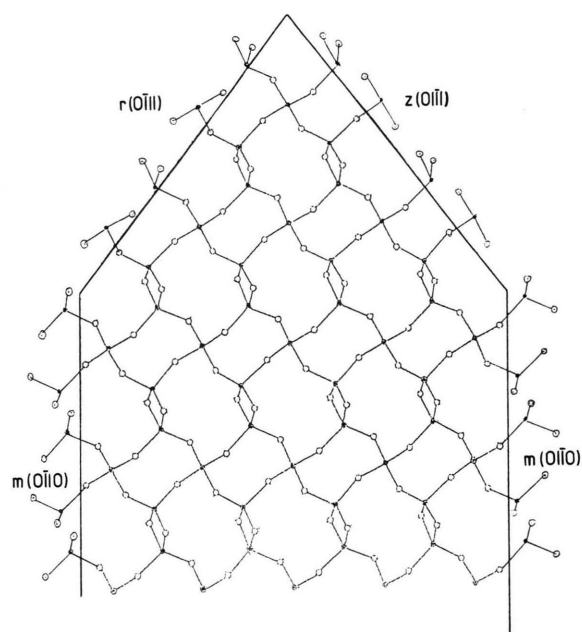


Fig. 1. Structure of trigonal quartz and its faces z , r , and m , taken from [2]. Projection perpendicular to the c -axis and parallel to two of the m -faces. ●:Silicium, ○:Oxygen. Possible positions of attaching SiO_2 units are shown outside the faces.

Reprint requests to Prof. Dr. A. Klemm, MPI für Chemie, Saarstr. 23, D-6500 Mainz.

0932-0784 / 90 / 1100-1374 \$ 01.30/0. – Please order a reprint rather than making your own copy.



Dieses Werk wurde im Jahr 2013 vom Verlag Zeitschrift für Naturforschung in Zusammenarbeit mit der Max-Planck-Gesellschaft zur Förderung der Wissenschaften e.V. digitalisiert und unter folgender Lizenz veröffentlicht: Creative Commons Namensnennung-Keine Bearbeitung 3.0 Deutschland Lizenz.

Zum 01.01.2015 ist eine Anpassung der Lizenzbedingungen (Entfall der Creative Commons Lizenzbedingung „Keine Bearbeitung“) beabsichtigt, um eine Nachnutzung auch im Rahmen zukünftiger wissenschaftlicher Nutzungsformen zu ermöglichen.

This work has been digitalized and published in 2013 by Verlag Zeitschrift für Naturforschung in cooperation with the Max Planck Society for the Advancement of Science under a Creative Commons Attribution-NoDerivs 3.0 Germany License.

On 01.01.2015 it is planned to change the License Conditions (the removal of the Creative Commons License condition “no derivative works”). This is to allow reuse in the area of future scientific usage.

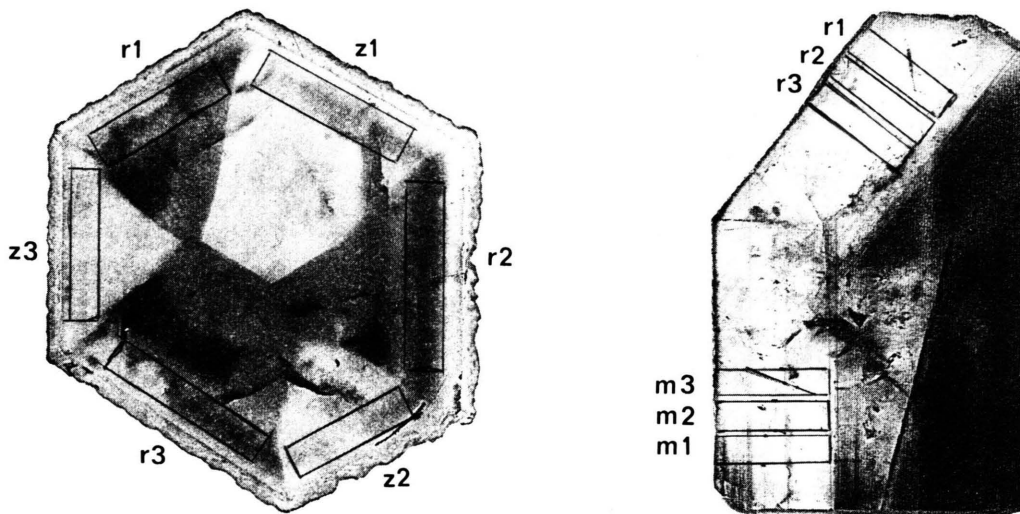


Fig. 2. Amethyst slices from which the probes were taken. *Crystal 1*: Slice perpendicular to *c*-axis through the *z* and *r* faces. Diameter ca. 45 mm, thickness 3 mm. The sector zoning is well visible. *Crystal 2*: Slice parallel to *c*-axis and perpendicular through *r* and *m* faces. Height 40 mm, thickness 3 mm. The mantle zoning is well visible.

etc.) from changes in colour. The inner and outer boundaries of the sample should be at a good distance from each other (several mm), because then an error in the positioning of the boundaries becomes less serious. All the opposing faces of a sample should be parallel to each other in order to secure equal contributions of the stratified material of the crystal to the sample, and the whole material of a sample must be carefully mixed before the analysis.

Experimental

We have chosen brazilian amethyst for our study, though it was not easy to find untwinned crystals with well developed *m* faces. The temperature of the hydrothermal formation of amethyst ranges from 70 to 285 °C [4]. Amethyst contains iron as impurity in the valence states Fe^{2+} and Fe^{3+} . The purple colour is caused by Fe^{4+} formed from Fe^{3+} by ionizing radiation [3, 5]. In order to deepen the colour, our crystals were γ -irradiated. 3 mm thick slices showed distinct mantle- and sector zones suitable for the positioning of samples (Figure 2).

Samples were cut by use of a diamond-saw. 20 mg aliquots of the carefully homogenized powders were taken for oxygen isotope analysis. For oxygen extraction a fluorination-technique was used, the resulting O_2 was converted to CO_2 . The fluorine was purified

Table 1. $\delta^{18}\text{O}$ of the probes shown in Fig. 2 and faces averaged values $\langle \delta^{18}\text{O} \rangle$.

Crystal 1			Crystal 2		
Probe	$\delta^{18}\text{O}$	$\langle \delta^{18}\text{O} \rangle$	Probe	$\delta^{18}\text{O}$	$\langle \delta^{18}\text{O} \rangle$
z1	26.9 ± 0.1	27.13	r1	16.5 ± 0.1	16.567
z2	27.6 ± 0.1		r2	16.6 ± 0.1	
z3	26.9 ± 0.1		r3	16.6 ± 0.1	
r1	27.1 ± 0.1	27.37	m1	17.0 ± 0.2	17.0
r2	27.5 ± 0.1		m2	17.1 ± 0.05	
r3	27.5 ± 0.1		m3	16.9 ± 0.05	

according to [6], which reduces blanks practically to zero. For mass spectrometric analysis a triple collector, 90°, 12 cm radius instruments (Sira-9, VG) was used. All samples were run in duplicate. These analyses were done by S.H.

Results and Discussion

We report here the results obtained from two crystals. Figure 2 illustrates the positions of sampling. The results are given in Table 1.

The δ values are defined as

$$\delta^{18}\text{O} = \left[\frac{(^{18}\text{O}/^{16}\text{O})}{(^{18}\text{O}/^{16}\text{O})_{\text{ST}}} - 1 \right] \cdot 10^3.$$

Table 2. Characteristics of the faces of amethyst.

Face	E_{att} [7] (kJ/mol)	Growth velocities v	Intensities of colour I	Fractionation factors α
z	1180.6			α_{r-z}
r	1137.9	$v_z > v_r$	$I_r > I_z$	$= 1.000234$
m	1056.2	$v_r > v_m$	$I_r > I_m$	α_{m-r} $= 1.000426$ $\alpha_{m-r} \cdot \alpha_{r-z}$ $= 1.000660$

The standard used to express ^{18}O enrichment or depletion is SMOW (standard mean ocean water).

The fractionation factor α is defined as

$$\alpha_{A-B} = (^{18}\text{O}/^{16}\text{O})_A / (^{18}\text{O}/^{16}\text{O})_B.$$

Two δ values and the respective fractionation factor α are related by

$$\alpha_{A-B} = (1 + \delta_A/1000) / (1 + \delta_B/1000).$$

The fractionation factors obtained from the face-averaged $\delta^{18}\text{O}$ values given in Table 1 are listed in Table 2

together with the attachment energies E_{att} of SiO_2 units on the faces z , r , and m resulting from calculations of Woensdregt [7], the relative velocities of growth of the faces, and their colouring [3]. Combination of the α_{m-r} and α_{r-z} values obtained from the crystals 2 and 1, respectively, gives $\alpha_{m-z} = 1.0007$ as the order of the fractionation factor between the faces m and z .

It is apparent that ^{18}O prefers the slower growing faces with their lower attachment energy of SiO_2 . The colouring does not follow this order but rather the order $m \rightarrow z \rightarrow r$ of increasing colour-intensity, a fact which is not yet understood. As for the observed isotope effect, the correspondence of growth-rate and attachment energy in the order z , r , m , where z has the highest attachment energy and the fastest growth-rate, with the lowest ability to concentrate ^{18}O suggests that there is a kinetic control of the face-controlled fractionation.

It can be expected that future work using high-resolution methods of O-isotope analysis (Laser-fluorination), will show that face controlled intracrystalline isotope fractionation is a general phenomenon.

- [1] D. Götz, K. Heinzinger, and A. Klemm, *Z. Naturforsch.* **30a**, 1667 (1975).
- [2] E. Dowty, *Amer. Mineralogist* **61**, 460 (1976).
- [3] R. Rykart, *Quarz-Monographie*, Ott Verlag, Thun, Schweiz, 1989.
- [4] W. H. Dennen and A. M. Puckett, *Can. Mineralogist* **11**, 448 (1972).

- [5] G. Lehmann and H. Bambauer, *Angew. Chem.* **85**, 281 (1973). – R. T. Cox, *J. Physics C, Solid State Phys.* **10**, 4613 (1977).
- [6] L. B. Asprey, *J. Fluorine Chem.* **7**, 359 (1976).
- [7] cf. P. Hartman, *Fortschr. Miner.* **57**, 2, 127 (1979).